

Analysis of integration site distributions and clonal abundances for gene therapy correction of cystinosis

John K. Everett, Ph.D. and Frederic Bushman, Ph.D.

April 2018

Contents

Summary of results	2
Human and mouse samples studied	2
UCSC browser exploration	2
Description of analysis techniques	3
Comparisons to previous trials	4
Integration events near oncogenes in human subjects	4
Integration events near oncogenes in mouse subjects	5
Mapping of integration site positions	6
Relative abundances of human subject samples	8
Expanded clones	10
Mouse transplant trials	11
References	21
Supplementary tables and figures	22
Numbers of inferred cells and integration sites identified in provided samples	22
Analyzed samples in which no integration sites were identified	24
Comparison of the number of integration sites and inferred cells	25
Integration positions of the lentiviral therapeutic vector from a previous WAS correction trial ¹ . .	26
Persistence of clones in mouse BM transplant trials	27
Sequencing depth	28

Summary of results

The goal of this analysis is to investigate the integration profile of a gene therapy vector for the correction of cystinosis in both mouse and human subjects and assess potential clonal expansions. The list of human oncogenes used throughout this analysis was compiled from the literature (link) and the list of mouse oncogenes was compiled from the retroviral tagged cancer gene database (RTCGD)¹ using an inclusion threshold of three or more incidents. The human oncogene list comprises 7.46% of all human genes (NCBI RefSeq) whereas the mouse oncogene list comprises 2.01% of all mouse genes. The frequency of integration sites in human subjects near oncogenes was not significantly different than a published trial using a comparable vector to correct Wiskott-Aldrich syndrome (WAS) from which no adverse events have been reported². The frequency of integration sites in bone marrow donor mice near oncogenes was generally less than that of mice in a previously published β -thalassemia mouse trial from which no adverse events have been reported³. The integration position profile for human subjects was very similar to that found in the WAS trial. The mouse bone marrow transplant trials yielded varying degrees of persistence in five of the nine trials where detection was limited due to both sequencing depth and vector copy number. No significant enrichment of integration events near oncogenes was identified between donor and recipient mice. The code base for this analysis is available on-line (link).

Human and mouse samples studied

Integration sites were detected in 74 samples from both human and mouse subjects (Tables 1 & S1) while no integration sites were detected in 10 of the provided samples (Table S2).

Table 1. Overview of data collection.

organism	samples	nReads	nFrag	nSites
human	30	19,834,249	132,619	93,050
mouse	44	22,064,342	91,576	5,346

UCSC browser exploration

UCSC browser sessions pre-loaded with the integration sites identified in this analysis are available via these links: (human subjects), (mouse subjects). You may have to allow your browser to open a new browser window. Integration sites are shown as blue (positive orientation integration) and red (reverse orientation integration) tick marks. For each integration site, a second track provides the maximum clonal abundance. Entering gene names into the search bar will direct the browser to specific genes.

Description of analysis techniques

We investigate effects of integration on cell growth using the following criteria: Integration Frequency is the frequency at which unique integration sites are observed in or near a given gene. Clonal Abundance is determined by quantifying the number of sites of linker ligation associated with each unique integration site. This samples the number of DNA chains at the start of the experiment allowing clonal expansion to be quantified⁴.

Relative clonal Abundance is determined per sample and is the percentage of identified cells attributed to a given clone. Integration sites and the clones harboring them are sampled from a larger population. It would be rare for all integration sites in a sample to be represented in the sequence data.

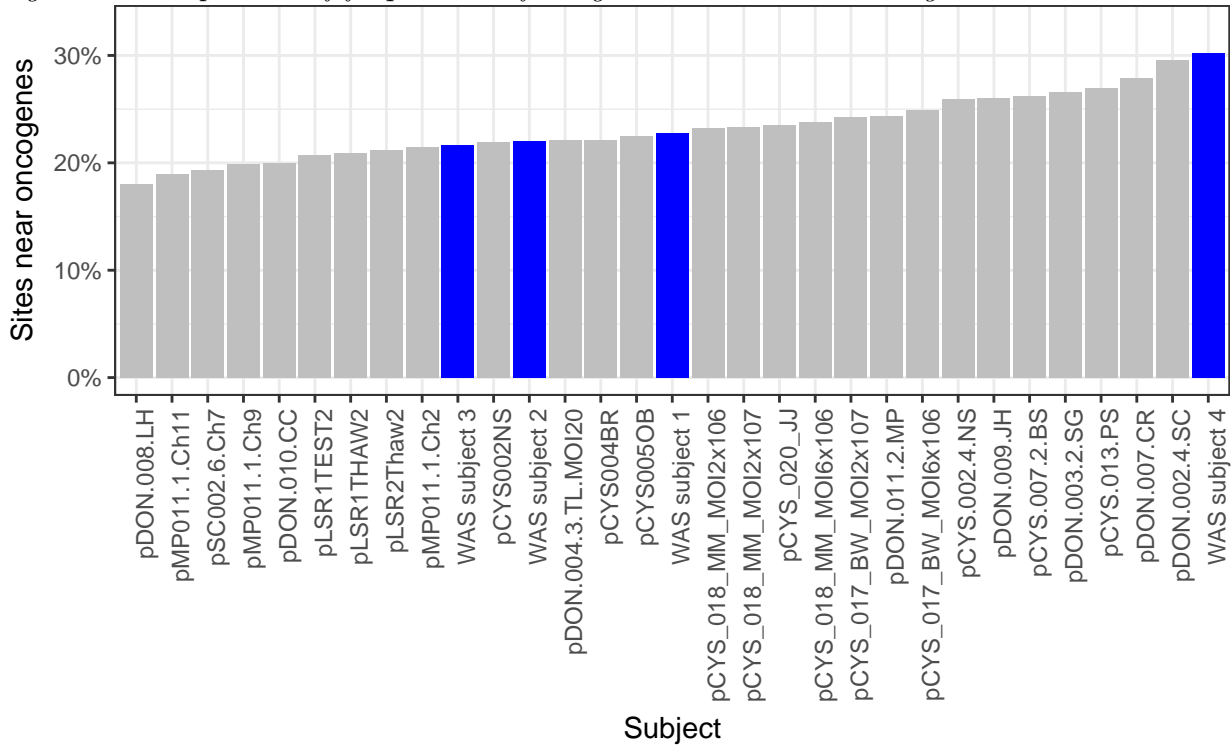
For this analysis, four technical replicates of each delivered sample were prepared, sequenced and analyzed with the INSPIRED integration site analysis pipeline (v1.2)⁵.

Comparisons to previous trials

Integration events near oncogenes in human subjects

In order to determine if the experimental vector has a higher propensity of integrating near suspected oncogene in humans than previously employed vectors, the frequency of integration near oncogenes was compared to a previously published human trial¹ which used a comparable lentiviral vector to correct Wiskott-Aldrich syndrome (WAS) where no adverse events have been reported to date. The frequency of integration near oncogenes in four WAS pre-transplant patient samples was compared to the frequency of integration in the experimental day 14 samples (Figure 1 [CYS: gray, WAS: blue]). The frequencies of integration near oncogenes of samples in this study and the previous WAS study were not significantly different (Mann-Whitney U-test p-value: 0.798).

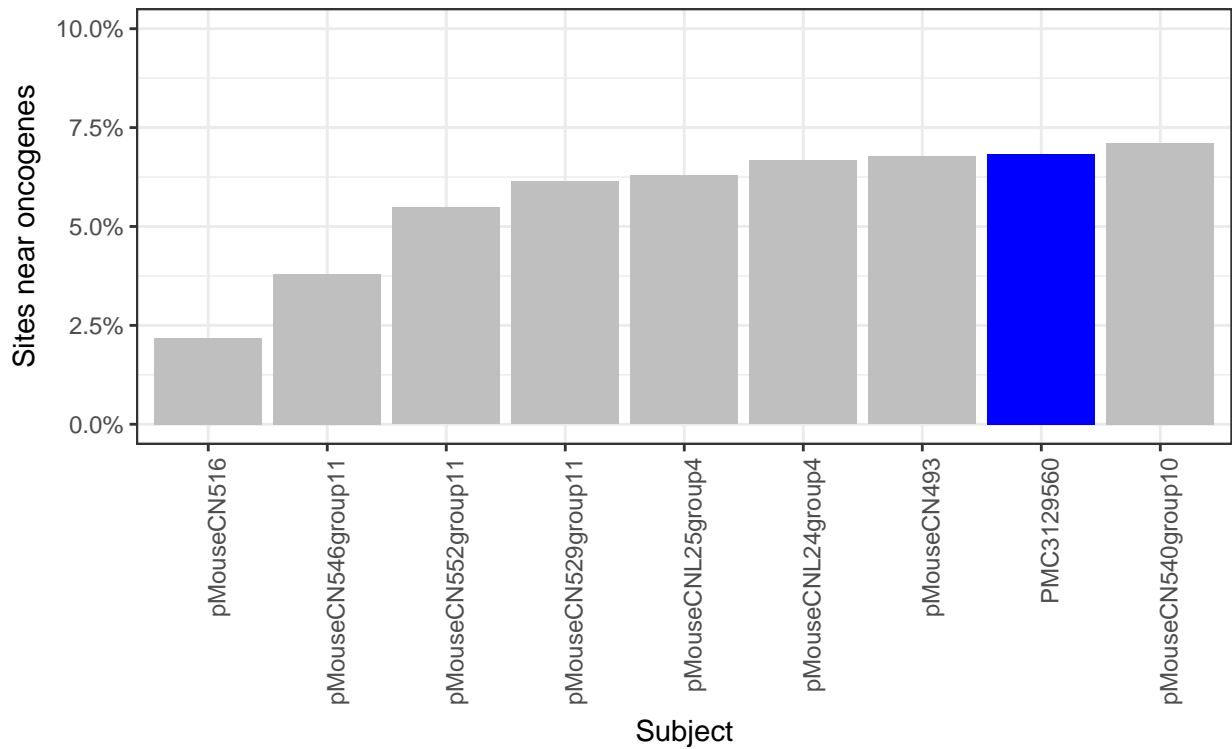
Figure 1. Comparison of frequencies of integration events near oncogenes.



Integration events near oncogenes in mouse subjects

In order to determine if the experimental vector has a higher propensity of integrating near suspected oncogene in mice than previously employed vectors, the frequency of integration near oncogenes was compared to a previously published mouse trial³ which used a comparable lentiviral vector to correct β -thalassemia. The frequency of integration events near onco genes in bone marrow donor mice was generally less than the mean frequency of integration events near oncogenes in the published trial (Figure 2 [CYS: gray, β -thalassemia trial: blue]).

Figure 2. Comparison of frequencies of integration events near oncogenes.



Mapping of integration site positions

Heat maps of identified integration sites are shown below in Figure 3a (human subjects) & 3b (mouse subjects). The integration position profile from human subjects is very similar to the profile from the previous WAS study (Figure S2).

Figure 3a

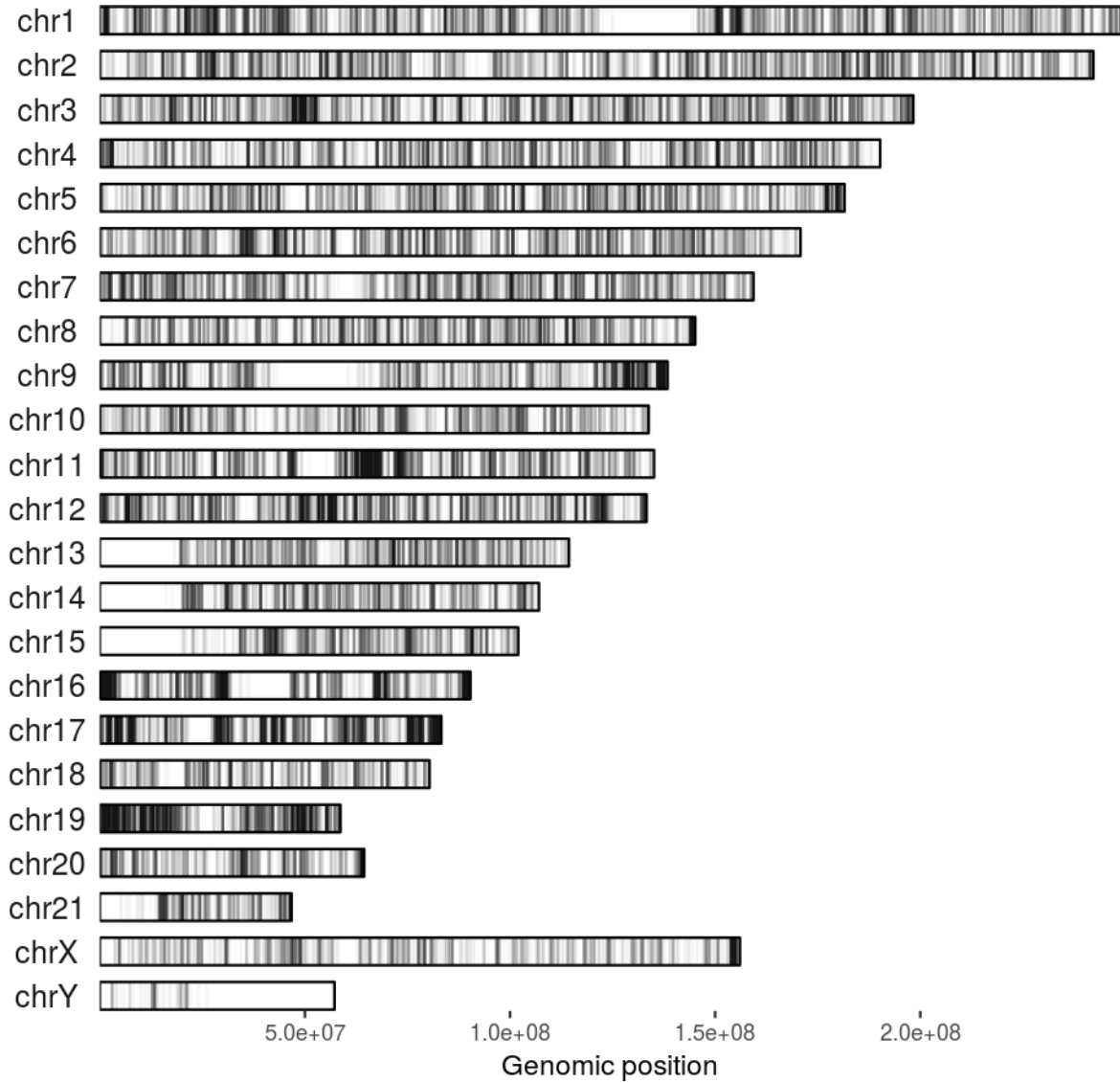
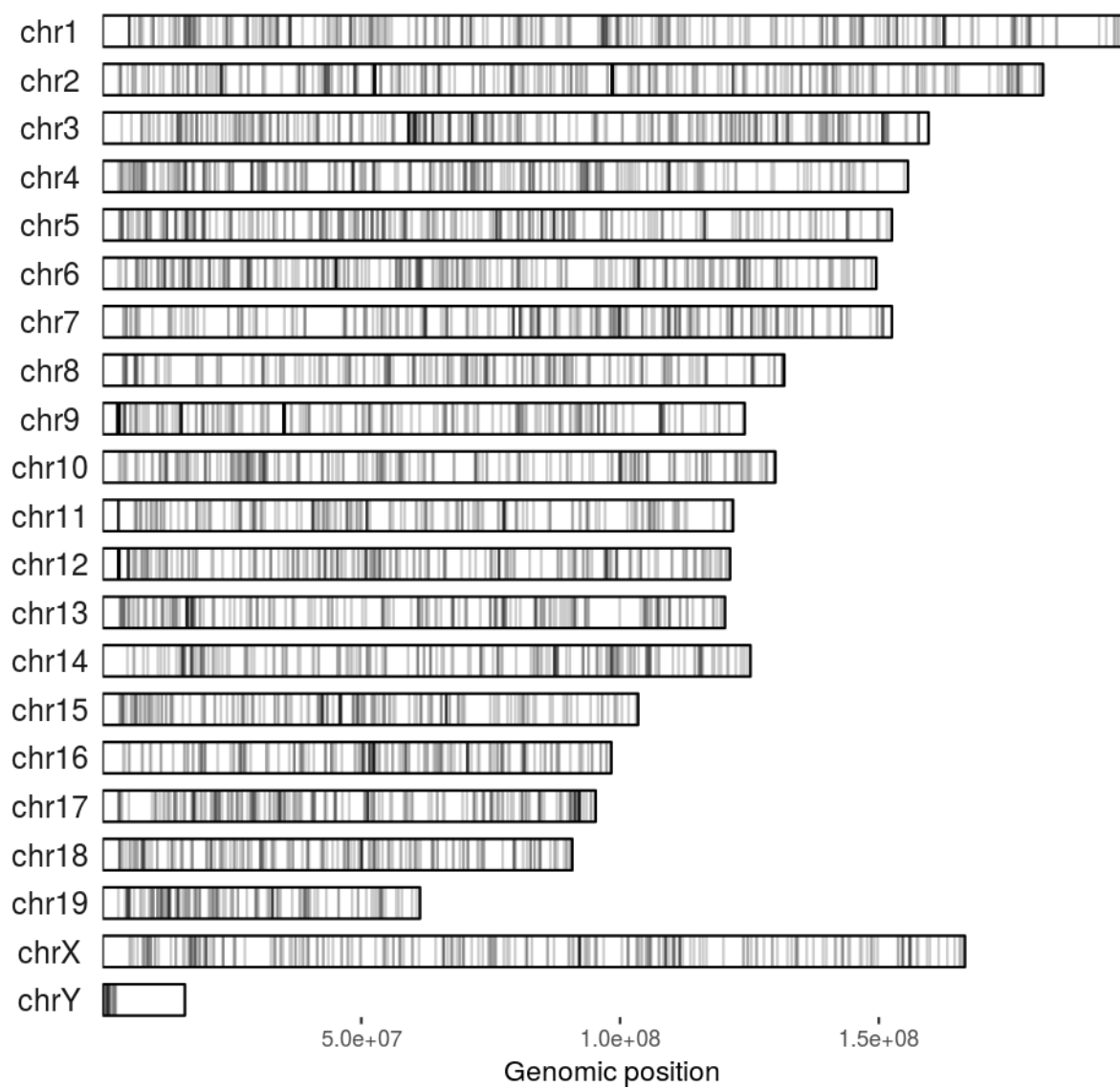


Figure 3b.



Relative abundances of human subject samples

The sample relative abundance plots below (Figure 4) show the most abundant 25 clones in each human sample as colored bars while less abundant clones were relegated to a single low abundance bar shown in gray. Subject DON.002.4.SC showed an expanded clone (30% relative abundance) with an integration event down stream of the non-coding RNA LOC105374704. Subject DON.007.CR showed an expanded clone (15% relative abundance) with three integration events within ZNF337. These two expanded clones are not of immediate concern given that such expanded clones appeared in the WAS trial used for comparison (Figure S1) and both samples contained relatively few inferred cells which inflate relative abundance values.

Figure 4.

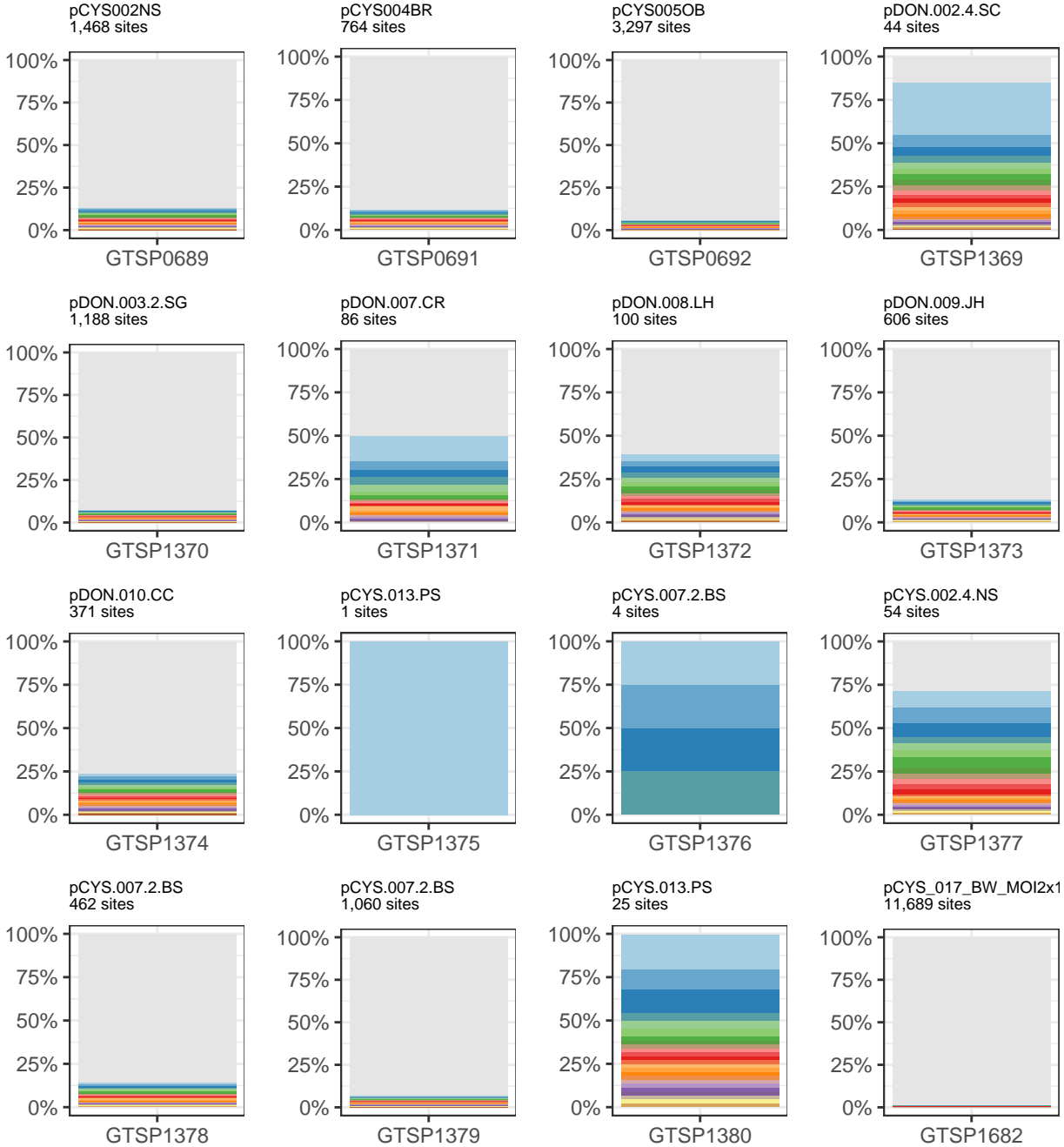


Figure 4. (continued)



Expanded clones

Table 2 below lists integration sites with relatives cell abundances $\geq 20\%$. These integration events may be driving cell division and follow-up longitudinal studies may be warranted. The estimated number of cells harboring each integration (estAbund) is shown for context.

Table 2.

patient	organism	timePoint	cellType	posid	relAbund	estAbund	nearestFeature
pDON.002.4.SC	human	D14	PB_CD34	chr5+30409434	29.92%	38	LOC105374704
pCYS.007.2.BS	human	D14	PBCD34-mock	chr1-218477558	25.00%	1	TGFB2
pCYS.007.2.BS	human	D14	PBCD34-mock	chr1-167962238	25.00%	1	DCAF6
pCYS.007.2.BS	human	D14	PBCD34-mock	chr6+11842138	25.00%	1	ADTRP
pCYS.007.2.BS	human	D14	PBCD34-mock	chr8+133682373	25.00%	1	LOC105375773
pCYS.013.PS	human	D14	PBCD34-mock	chr12+82136325	100.00%	1	LOC101928449
pCYS.013.PS	human	D14	PBCD34-MOI40	chr8+67244348	20.45%	9	ARFGEF1
pMouseCNL24group4	mouse	M6	Mouse_BM	chr2+141127890	37.44%	1796	MacroD2
pMouseCNL23group4control	mouse	M6	Mouse_BM	chr3-59165408	33.33%	2	Igsf10
pMouseCNL25group4	mouse	M6	Mouse_BM	chr3-59165408	32.30%	2907	Igsf10
pMouseCNL25group4	mouse	M6	Mouse_BM	chr3+71430357	21.19%	1907	Gm6634
pMouseCNL25group4	mouse	M6	Mouse_BM	chr9+15188460	20.42%	1838	Cep295
pMouseCNL24group4	mouse	M6	Mouse_BM	chr18-79750998	25.58%	1227	Setbp1
pMouseCNL24group4	mouse	M6	Mouse_BM	chrX+48224394	24.70%	1185	Stk26
pMouseCNL38group1A	mouse	M6	Mouse_BM	chr7-115316991	50.00%	1	Olfr486
pMouseCNL38group1A	mouse	M6	Mouse_BM	chr14-102130900	50.00%	1	Lmo7
pMouseCN493	mouse	M6	Mouse_BM	chr14+15556797	21.72%	1769	Slc4a7
pMouseCNL59	mouse	M6	Mouse_BM	chr2+52586806	25.16%	525	Stam2
pMouseCNL58	mouse	M6	Mouse_BM	chr2+141127890	100.00%	3	MacroD2
pMouseCNL59	mouse	M6	Mouse_BM	chr3-59165408	33.06%	690	Igsf10
pMouseCN493	mouse	M6	Mouse_BM	chr6-10697710	26.54%	2161	AA545190
pMouseCNL53	mouse	M6	Mouse_BM	chr19+18123881	100.00%	1	Pcsk5
pMouseCN493	mouse	M6	Mouse_BM	chrX-111592392	29.17%	2375	Klhl4
pMouseCN545group11	mouse	M6	Mouse_BM	chr5-12432693	39.48%	2080	Sema3d
pMouseCN545group11	mouse	M6	Mouse_BM	chr18-15129653	44.06%	2321	Kctd1
pCNL80	mouse	M6	Mouse_BM	chr3+123970190	32.46%	37	Tram111
pCNL82	mouse	M6	Mouse_BM	chr10-40246905	50.00%	1	Slc22a16
pCNL82	mouse	M6	Mouse_BM	chr10+94767778	50.00%	1	Cradd
pCNL59	mouse	M6	Bone Marrow	chr2+52586806	37.50%	33	Stam2
pCNL59	mouse	M6	Bone Marrow	chr2+52586806	26.47%	18	Stam2
pCNL59	mouse	M6	B Cells	chr2+52586806	38.89%	7	Stam2
pCNL59	mouse	M6	Bone Marrow	chr3-59165408	25.00%	22	Igsf10
pCNL59	mouse	M6	Bone Marrow	chr3-59165408	30.88%	21	Igsf10
pCNL59	mouse	M6	B Cells	chr3+71430357	27.78%	5	Gm6634
pCNL59	mouse	M6	Bone Marrow	chr9+15188460	23.86%	21	Cep295
pCNL59	mouse	M6	Bone Marrow	chr9+15188460	29.41%	20	Cep295
pCNL59	mouse	M6	B Cells	chr9+15188460	27.78%	5	Cep295
pCN760	mouse	6M	Bone Marrow	chr1-99613407	25.00%	4	Ppip5k2
pCN774	mouse	6M	Bone Marrow	chr1-21011655	20.09%	90	Tram2
pCN803	mouse	6M	Bone Marrow	chr3+60155698	25.07%	565	Mbnl1
pCN803	mouse	6M	Bone Marrow	chr14-105778668	24.76%	558	5430440P10Rik

Mouse transplant trials

The positions of identified integration sites from cell transplant trials with nine pairs of mice are shown in Figure 5a (donor mice) and Figure 5b (recipient mice). The gRxCluster software package did not identify clusters of integration sites between donor and recipient mice with a false discovery rate of $\leq 10\%$. The relative clonal abundances of samples from the transplant trials are shown in Figure 6 where donor mice are shown on the left and recipient mice are shown on the right. Integration sites are denoted by both nearest gene and genomic coordinate and annotated with an asterisk (*) if located within transcription units and with a tilde (~) if the nearest gene is considered an oncogene. Below each abundance plot is a Fisher's exact test for the enrichment of oncogenes. None of the tests returned a significant result. The clonal abundances of clones found in both donor and recipient mice is shown in Table S3. The identification of relatively few persistent clones is likely due to sequencing experiments sampling only a subset of existing integration sites and a number of samples with low vector copy numbers (Figures 5B & S3).

Figure 5

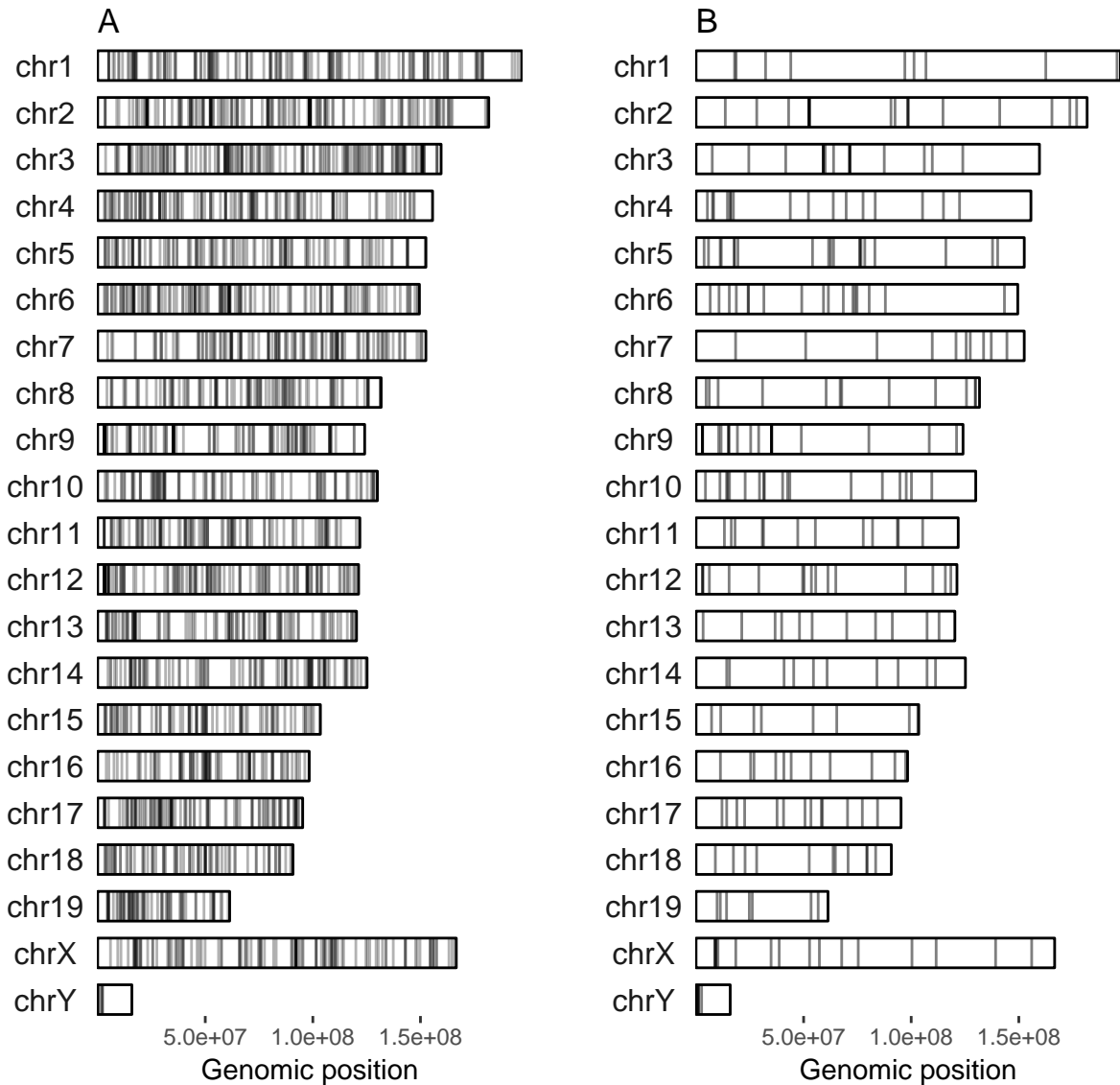
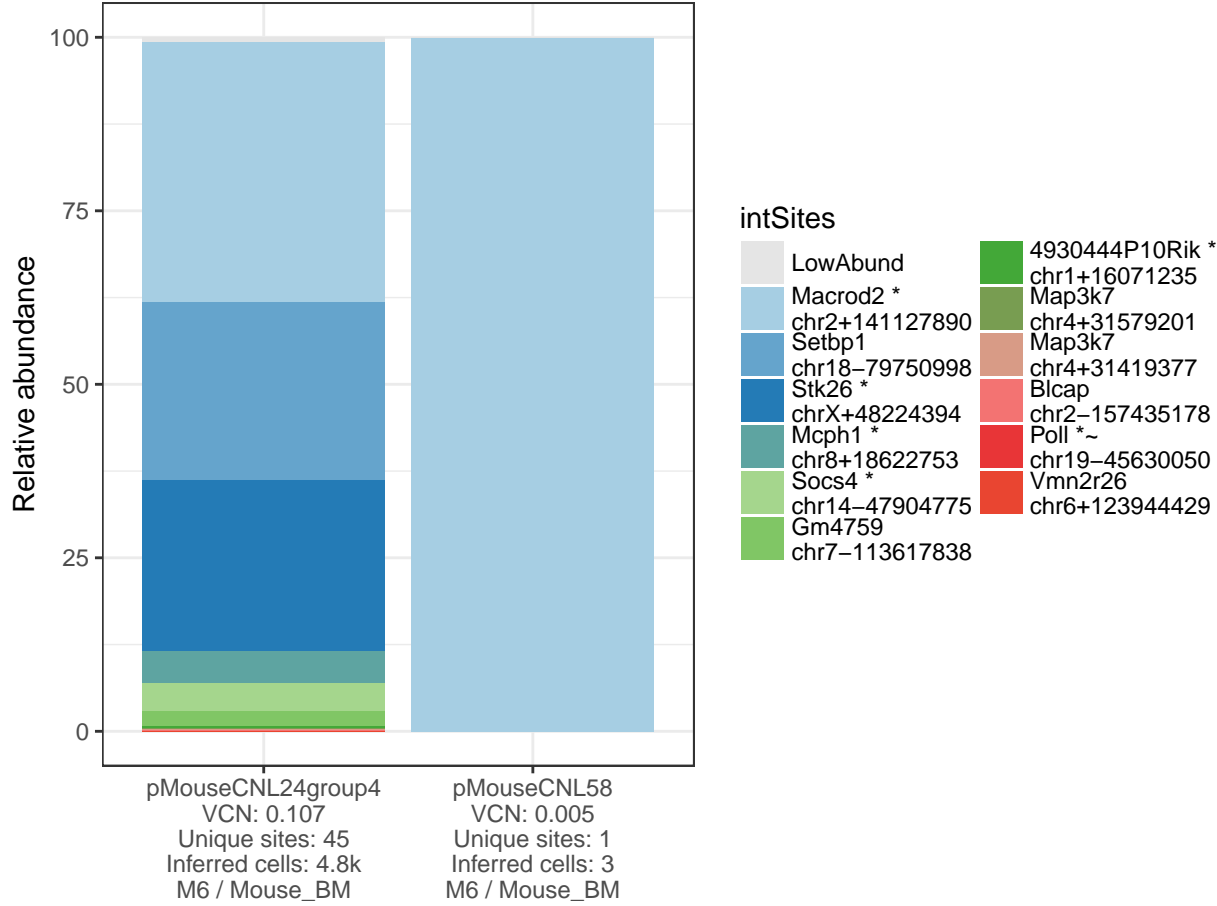


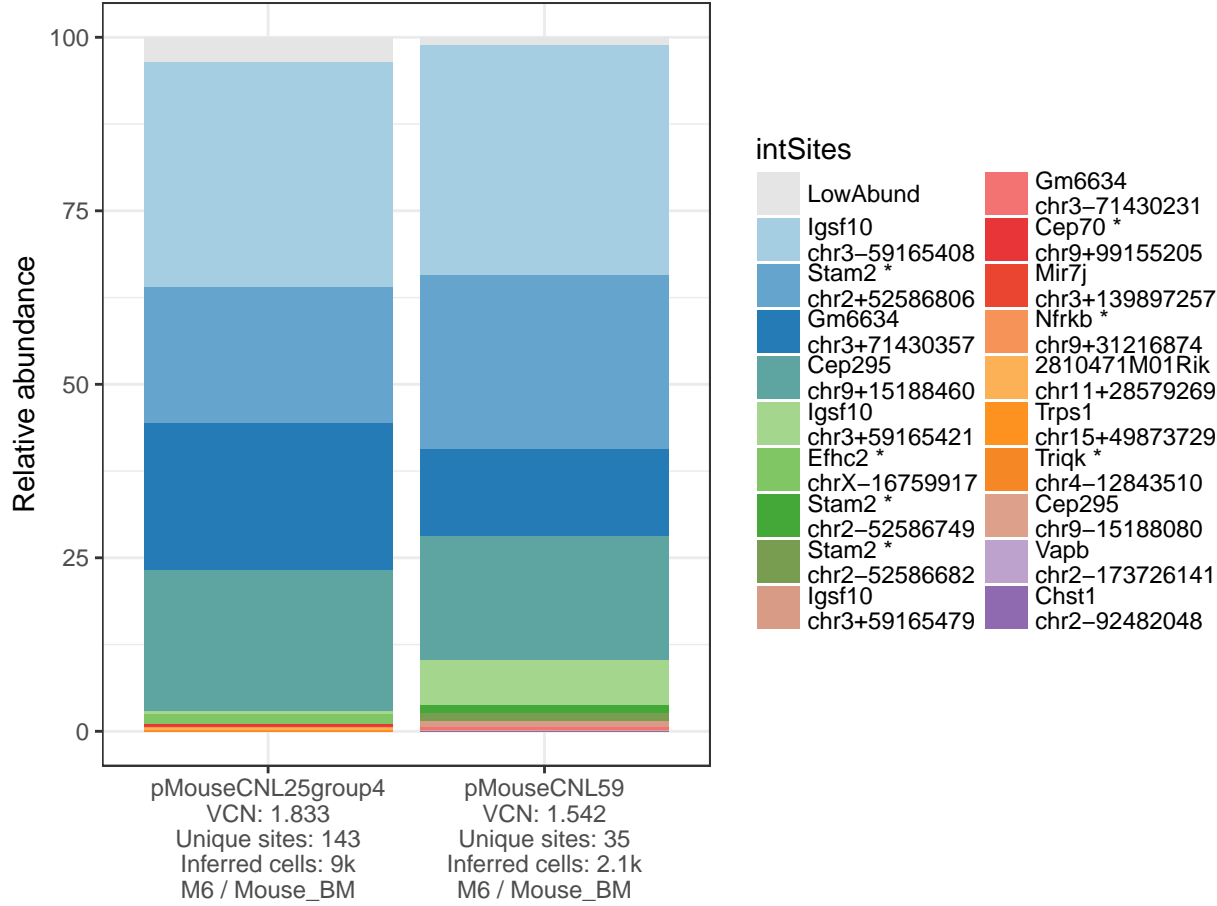
Figure 6a.



Sites near oncogenes, Fisher's exact p-value: 1.000

	Not near onco	Near onco
pMouseCNL24group4	42	3
pMouseCNL58	1	0

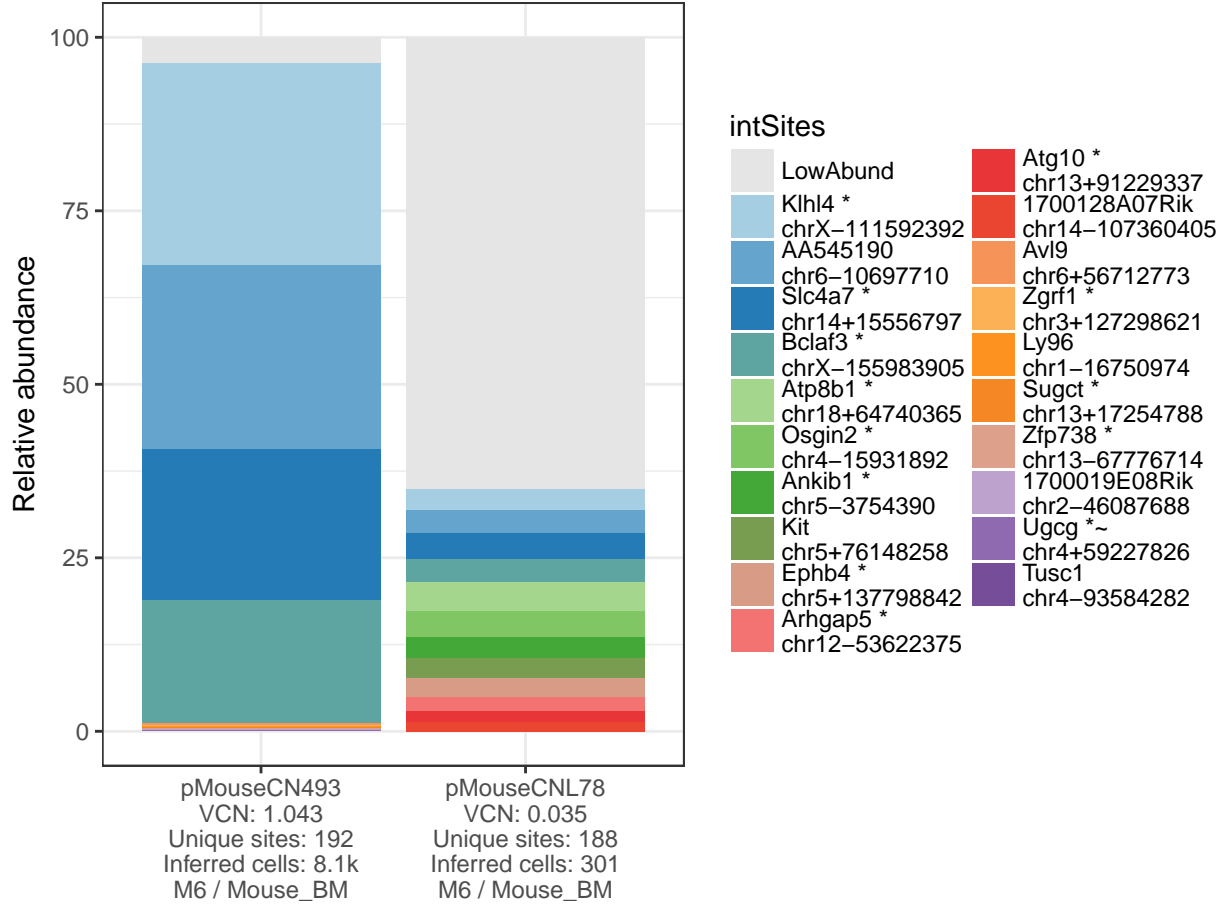
Figure 6b.



Sites near oncogenes, Fisher's exact p-value: 0.208

	Not near onco	Near onco
pMouseCNL25group4	134	9
pMouseCNL59	35	0

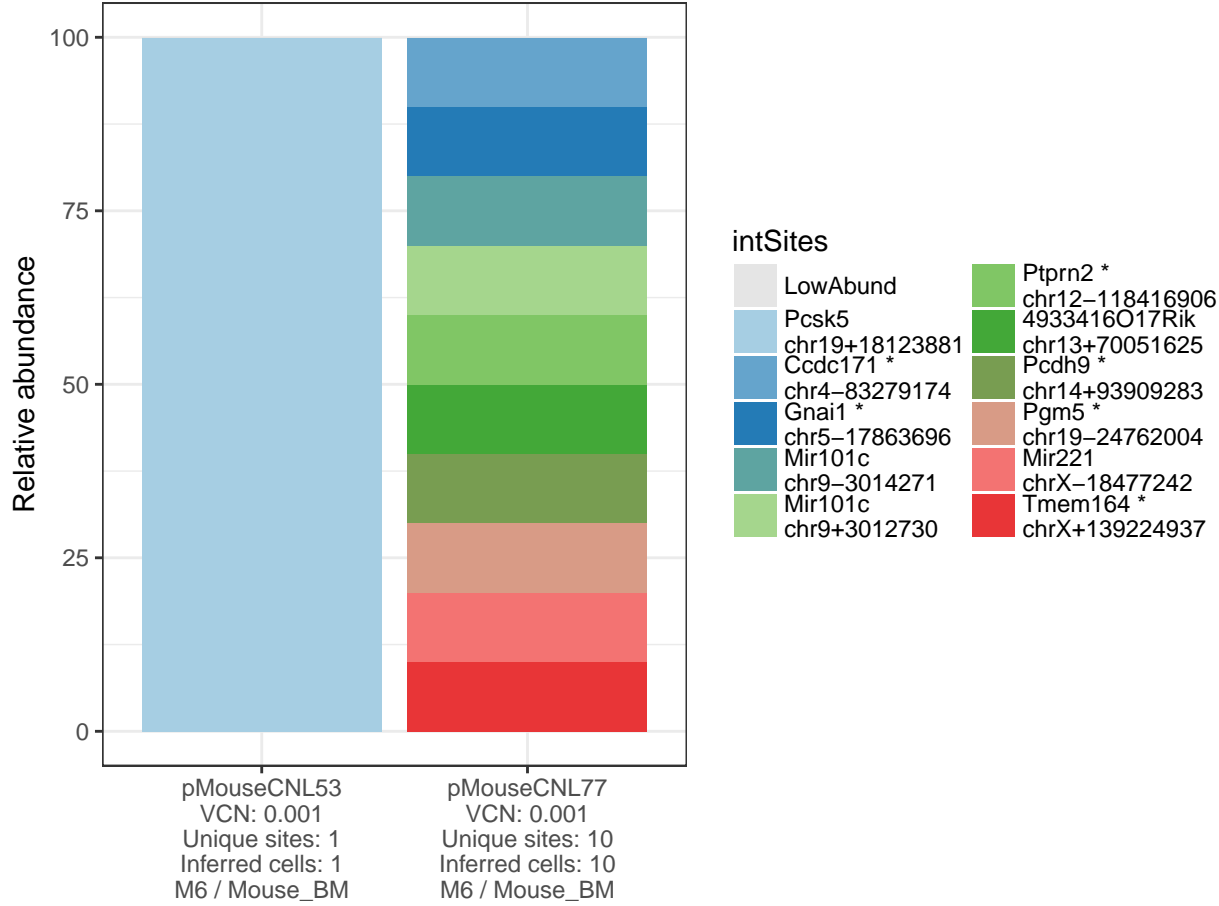
Figure 6c.



Sites near oncogenes, Fisher's exact p-value: 0.647

	Not near onco	Near onco
pMouseCN493	179	12
pMouseCNL78	159	8

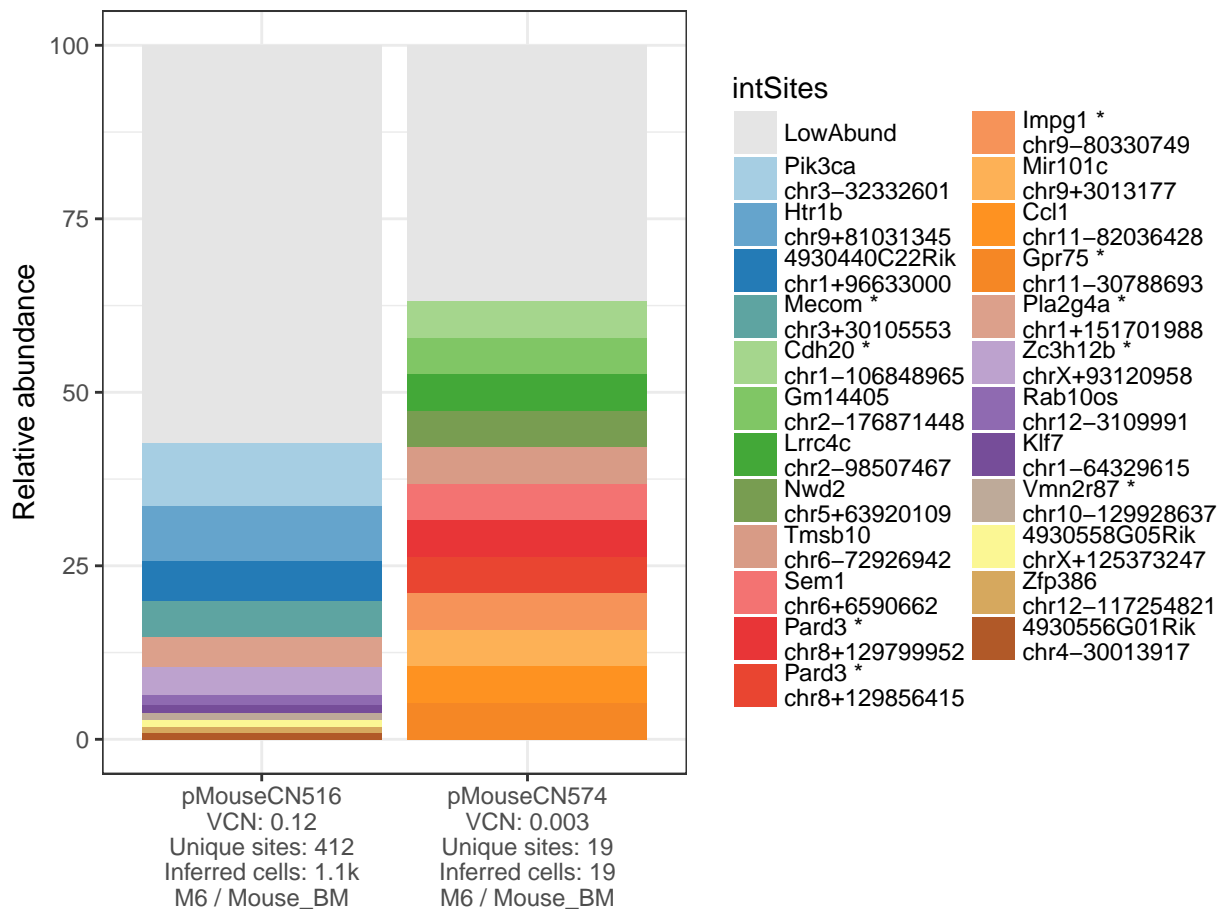
Figure 6d.



Sites near oncogenes, Fisher's exact p-value: 1.000

	Not near onco	Near onco
pMouseCNL53	1	0
pMouseCNL77	10	0

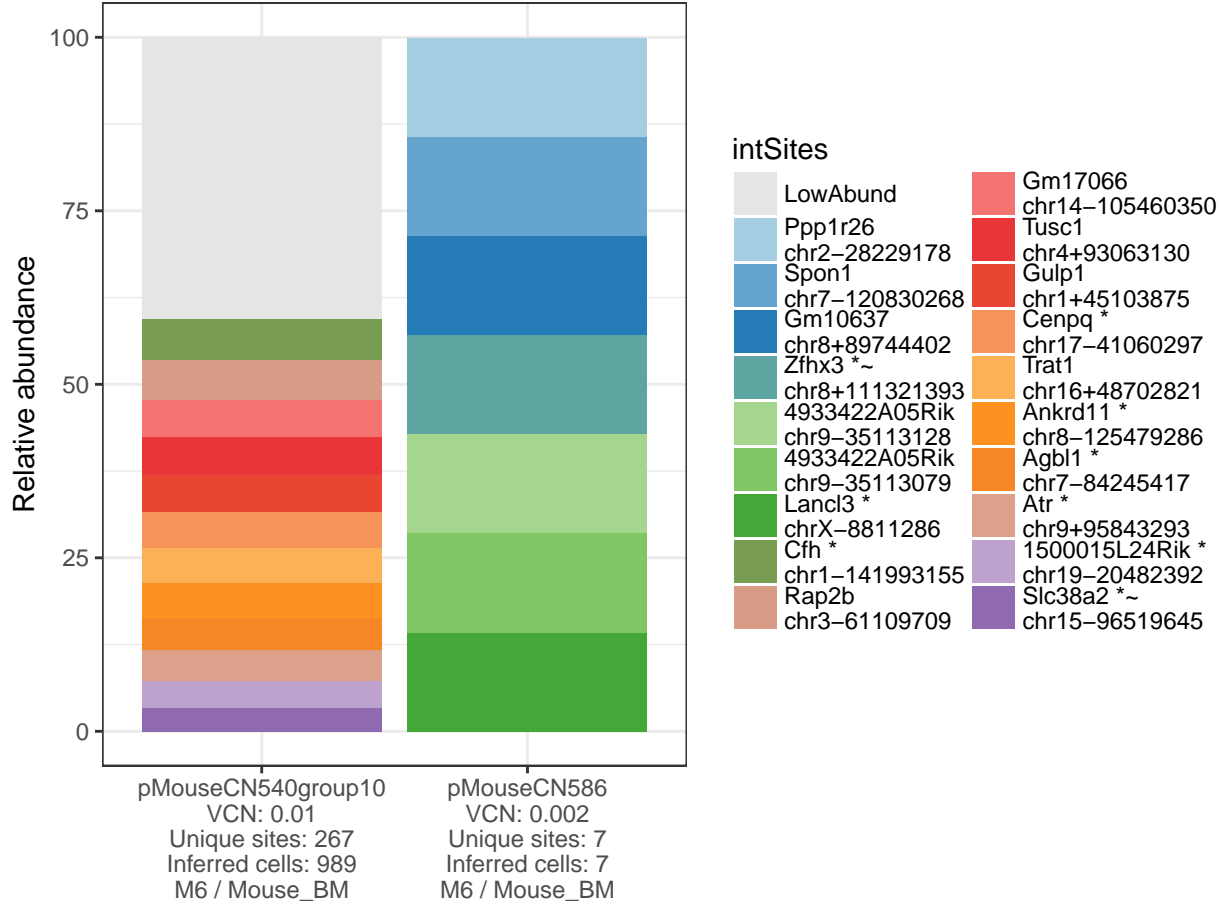
Figure 6e.



Sites near oncogenes, Fisher's exact p-value: 1.000

	Not near onco	Near onco
pMouseCN516	392	8
pMouseCN574	18	0

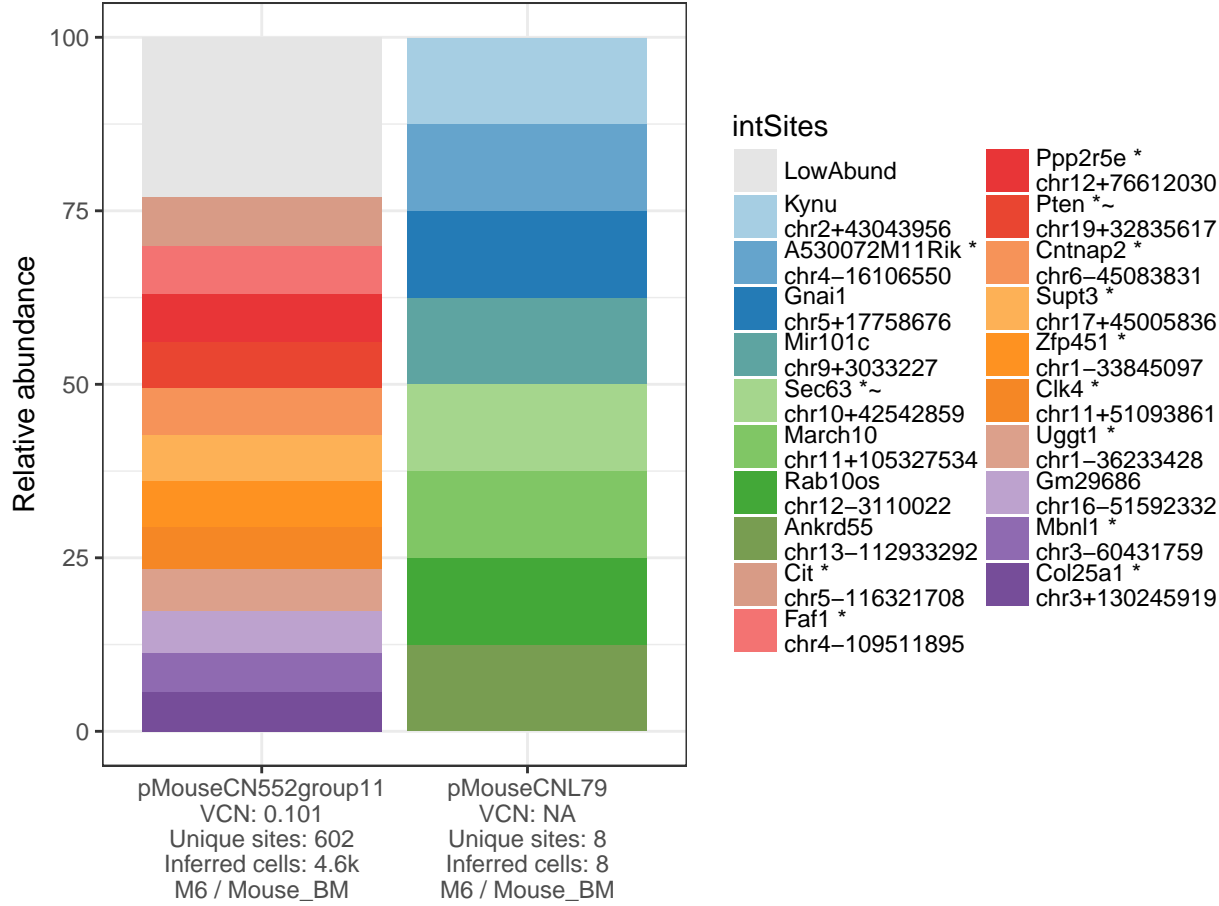
Figure 6f.



Sites near oncogenes, Fisher's exact p-value: 0.415

	Not near onco	Near onco
pMouseCN540group10	248	19
pMouseCN586	6	1

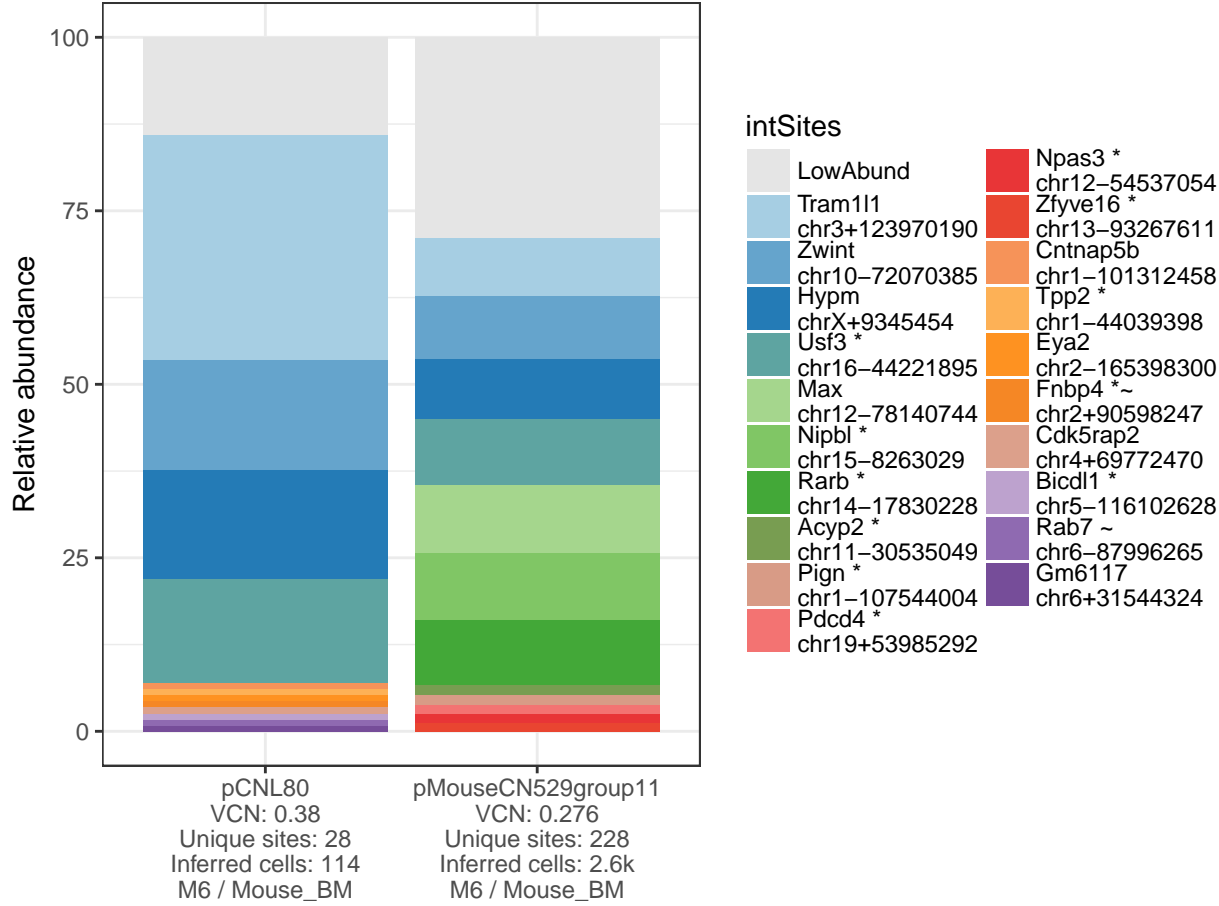
Figure 6g.



Sites near oncogenes, Fisher's exact p-value: 0.366

	Not near onco	Near onco
pMouseCN552group11	559	32
pMouseCNL79	7	1

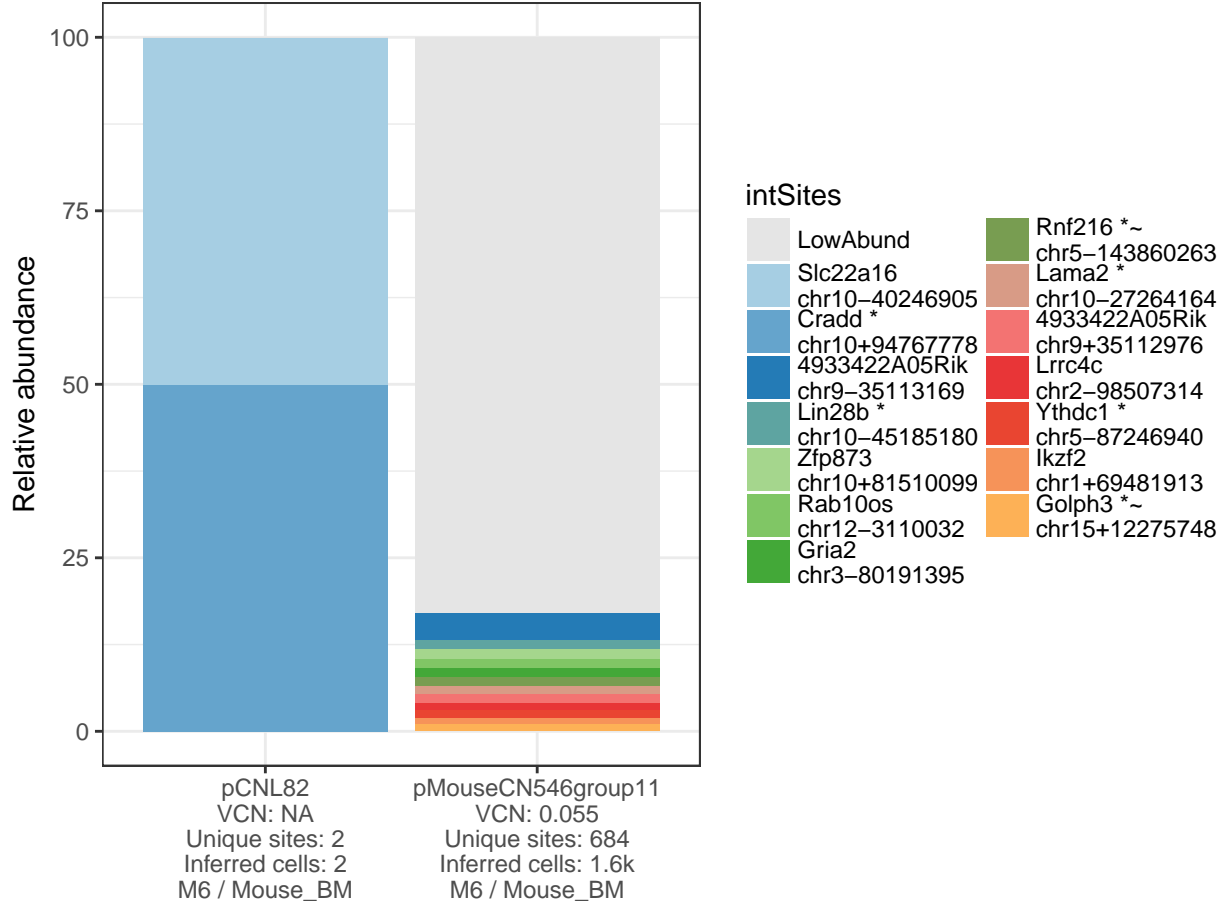
Figure 6h.



Sites near oncogenes, Fisher's exact p-value: 0.673

	Not near onco	Near onco
pMouseCN529group11	214	13
pCNL80	26	2

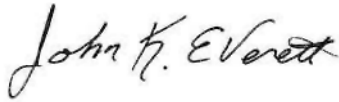
Figure 6i.



Sites near oncogenes, Fisher's exact p-value: 1.000

	Not near onco	Near onco
pMouseCN546group11	646	25
pCNL82	2	0

Analyst



John K. Everett, Ph.D.

Laboratory director



Frederic D. Bushman, Ph.D.

References

1. RTCGD: retroviral tagged cancer gene database. Akagi K, Suzuki T, Stephens RM, Jenkins NA, Copeland NG. *Nucleic Acids Res.* 2004 Jan 1;32(Database issue):D523-7.
2. Outcomes following gene therapy in patients with severe Wiskott-Aldrich syndrome. Hacein-Bey Abina S, Gaspar HB, Blondeau J, Caccavelli L, Charrier S, Buckland K, Picard C, Six E, Himoudi N, Gilmour K, McNicol AM, Hara H, Xu-Bayford J, Rivat C, Touzot F, Mavilio F, Lim A, Treluyer JM, Héritier S, Lefrère F, Magalon J, Pengue-Koyi I, Honnet G, Blanche S, Sherman EA, Male F, Berry C, Malani N, Bushman FD, Fischer A, Thrasher AJ, Galy A, Cavazzana M. *JAMA.* 2015 Apr 21;313(15):1550-63.
3. Distribution of Lentiviral Vector Integration Sites in Mice Following Therapeutic Gene Transfer to Treat β -thalassemia. Ronen K, Negre O, Roth S, Colomb C, Malani N, Denaro M, Brady T, Fusil F, Gillet-Legrand B, Hehir K, Beuzard Y, Leboulch P, Down JD, Payen E, Bushman FD. *Mol Ther.* 2011 Jul;19(7):1273-86.
4. Estimating abundances of retroviral insertion sites from DNA fragment length data. Berry CC, Gillet NA, Melamed A, Gormley N, Bangham CR, Bushman FD. *Bioinformatics.* 2012 Mar 15;28(6):755-62.
5. INSPIRED: A Pipeline for Quantitative Analysis of Sites of New DNA Integration in Cellular Genomes. Sherman E, Nobles C, Berry CC, Six E, Wu Y, Dryga A, Malani N, Male F, Reddy S, Bailey A, Bittinger K, Everett JK, Caccavelli L, Drake MJ, Bates P, Hacein-Bey-Abina S, Cavazzana M, Bushman FD. *Mol Ther Methods Clin Dev.* 2016 Dec 18;4:39-49.

Supplementary tables and figures

Numbers of inferred cells and integration sites identified in provided samples

Table S1.

organism	GTSP	Subject	Cell type	VCN	Time point	Number inferred cells	Number of intSites
human	GTSP0689	pCYS002NS	PBCD34-MOI20	0.940	D14	2,978	1,468
human	GTSP0691	pCYS004BR	PBCD34-MOI20	0.930	D14	1,034	764
human	GTSP0692	pCYS005OB	PB_CD34	0.970	D14	8,384	3,297
human	GTSP1369	pDON.002.4.SC	PB_CD34	4.520	D14	127	44
human	GTSP1370	pDON.003.2.SG	PB_CD34	2.440	D14	1,482	1,188
human	GTSP1371	pDON.007.CR	PB_CD34	1.270	D14	122	86
human	GTSP1372	pDON.008.LH	PB_CD34	2.530	D14	124	100
human	GTSP1373	pDON.009.JH	PB_CD34	5.280	D14	757	606
human	GTSP1374	pDON.010.CC	PB_CD34	3.290	D14	513	371
human	GTSP1375	pCYS.013.PS	PBCD34-mock	NA	D14	1	1
human	GTSP1376	pCYS.007.2.BS	PBCD34-mock	0.002	D14	4	4
human	GTSP1377	pCYS.002.4.NS	PB_CD34	2.400	D14	102	54
human	GTSP1378	pCYS.007.2.BS	PBCD34-MOI20	3.640	D14	543	462
human	GTSP1379	pCYS.007.2.BS	PBCD34-MOI40	6.100	D14	1,210	1,060
human	GTSP1380	pCYS.013.PS	PBCD34-MOI40	1.000	D14	44	25
human	GTSP1682	pCYS_017_BW_MOI2x107	PB_CD34	1.660	D14	16,696	11,689
human	GTSP1683	pCYS_017_BW_MOI6x106	PB_CD34	1.415	D14	16,690	11,090
human	GTSP1685	pCYS_018_MM_MOI2x107	PB_CD34	0.958	D14	11,679	8,444
human	GTSP1686	pCYS_018_MM_MOI6x106	PB_CD34	0.530	D14	7,089	4,547
human	GTSP1687	pCYS_018_MM_MOI2x106	PB_CD34	0.331	D14	3,594	2,508
human	GTSP1688	pCYS_020_JJ	PB_CD34	2.590	D14	21,709	14,755
human	GTSP1689	pMP011.1.Ch2	PB_CD34	1.607	D14	1,500	940
human	GTSP1690	pSC002.6.Ch7	PB_CD34	2.350	D14	401	222
human	GTSP1691	pMP011.1.Ch9	PB_CD34	2.420	D14	692	427
human	GTSP1692	pMP011.1.Ch11	PB_CD34	1.074	D14	596	353
human	GTSP1694	pDON.004.3.TL.MOI20	PB_CD34	3.250	D14	5,273	4,569
human	GTSP1695	pDON.011.2.MP	PB_CD34	3.950	D14	11,199	7,065
human	GTSP1969	pLSR1TEST2	BM CD34+ Cells	0.695	0	2,568	2,215
human	GTSP1970	pLSR1THAW2	BM CD34+ Cells	0.709	0	6,320	6,009
human	GTSP1971	pLSR2Thaw2	BM CD34+ Cells	1.020	0	9,188	8,687

Table S1 (continued).

organism	GTSP	Subject	Cell type	VCN	Time point	Number inferred cells	Number of intSites
mouse	GTSP0829	pMouseCNL23group4control	Mouse_BM	NA	M6	6	5
mouse	GTSP0830	pMouseCNL24group4	Mouse_BM	0.107	M6	4,797	45
mouse	GTSP0831	pMouseCNL25group4	Mouse_BM	1.833	M6	9,000	143
mouse	GTSP0832	pMouseCNL38group1A	Mouse_BM	NA	M6	2	2
mouse	GTSP0833	pMouseCulture	Mouse_Scalpos	2.760	D14	80	28
mouse	GTSP0891	pMouseCN493	Mouse_BM	1.043	M6	8,143	192
mouse	GTSP0892	pMouseCNL53	Mouse_BM	0.001	M6	1	1
mouse	GTSP0947	pMouseCNL58	Mouse_BM	0.005	M6	3	1
mouse	GTSP0948	pMouseCNL59	Mouse_BM	1.542	M6	2,087	35
mouse	GTSP0949	pMouseCN516	Mouse_BM	0.120	M6	1,108	412
mouse	GTSP0950	pMouseCN518	Mouse_BM	2.430	M6	3,399	103
mouse	GTSP1079	pMouseCN540group10	Mouse_BM	0.010	M6	989	267
mouse	GTSP1080	pMouseCN552group11	Mouse_BM	0.101	M6	4,636	602
mouse	GTSP1081	pMouseCN529group11	Mouse_BM	0.276	M6	2,610	228
mouse	GTSP1082	pMouseCN545group11	Mouse_BM	1.798	M6	5,268	35
mouse	GTSP1083	pMouseCN546group11	Mouse_BM	0.055	M6	1,603	684
mouse	GTSP1084	pMouseCNL70group12	Mouse_BM	NA	M6	1,121	94
mouse	GTSP1146	pMouseCN557	Mouse_BM	1.597	M6	14,244	745
mouse	GTSP1147	pMouseCNL77	Mouse_BM	0.001	M6	10	10
mouse	GTSP1148	pMouseCNL78	Mouse_BM	0.035	M6	301	188
mouse	GTSP1149	pMouseCN574	Mouse_BM	0.003	M6	19	19
mouse	GTSP1150	pMouseCN586	Mouse_BM	0.002	M6	7	7
mouse	GTSP1151	pMouseCNL79	Mouse_BM	NA	M6	8	8
mouse	GTSP1481	pCNL80	Mouse_BM	0.380	M6	114	28
mouse	GTSP1482	pCNL82	Mouse_BM	NA	M6	2	2
mouse	GTSP1696	pCN665	Mouse_BM	4.490	M6	3,706	190
mouse	GTSP1697	pCN671	Mouse_BM	0.486	M6	5,515	247
mouse	GTSP1705	pCN552	Bone Marrow	NA	M6	63	15
mouse	GTSP1706	pCN552	T-Cells	NA	M6	174	49
mouse	GTSP1707	pCN552	B Cells	NA	M6	865	161
mouse	GTSP1708	pCN552	Bone Marrow	NA	M6	467	104
mouse	GTSP1709	pCNL59	Bone Marrow	NA	M6	88	6
mouse	GTSP1710	pCNL59	Bone Marrow	NA	M6	68	5
mouse	GTSP1712	pCNL59	B Cells	NA	M6	18	4
mouse	GTSP1867	pCN746	Bone Marrow	NA	M6	141	34
mouse	GTSP1972	pCN752	Bone Marrow	0.004	6M	225	74
mouse	GTSP1973	pCN755	Bone Marrow	NA	6M	28	27
mouse	GTSP1974	pCN760	Bone Marrow	0.001	6M	16	10
mouse	GTSP1977	pCN774	Bone Marrow	0.039	6M	448	191
mouse	GTSP1978	pCN801	Bone Marrow	10.490	6M	15,278	102
mouse	GTSP1979	pCN803	Bone Marrow	0.654	6M	2,254	149
mouse	GTSP1980	pCN804	Bone Marrow	0.003	6M	68	28
mouse	GTSP1981	pCN806	Bone Marrow	0.001	6M	8	8
mouse	GTSP1982	pCN809	Bone Marrow	0.572	6M	2,588	101

Analyzed samples in which no integration sites were identified

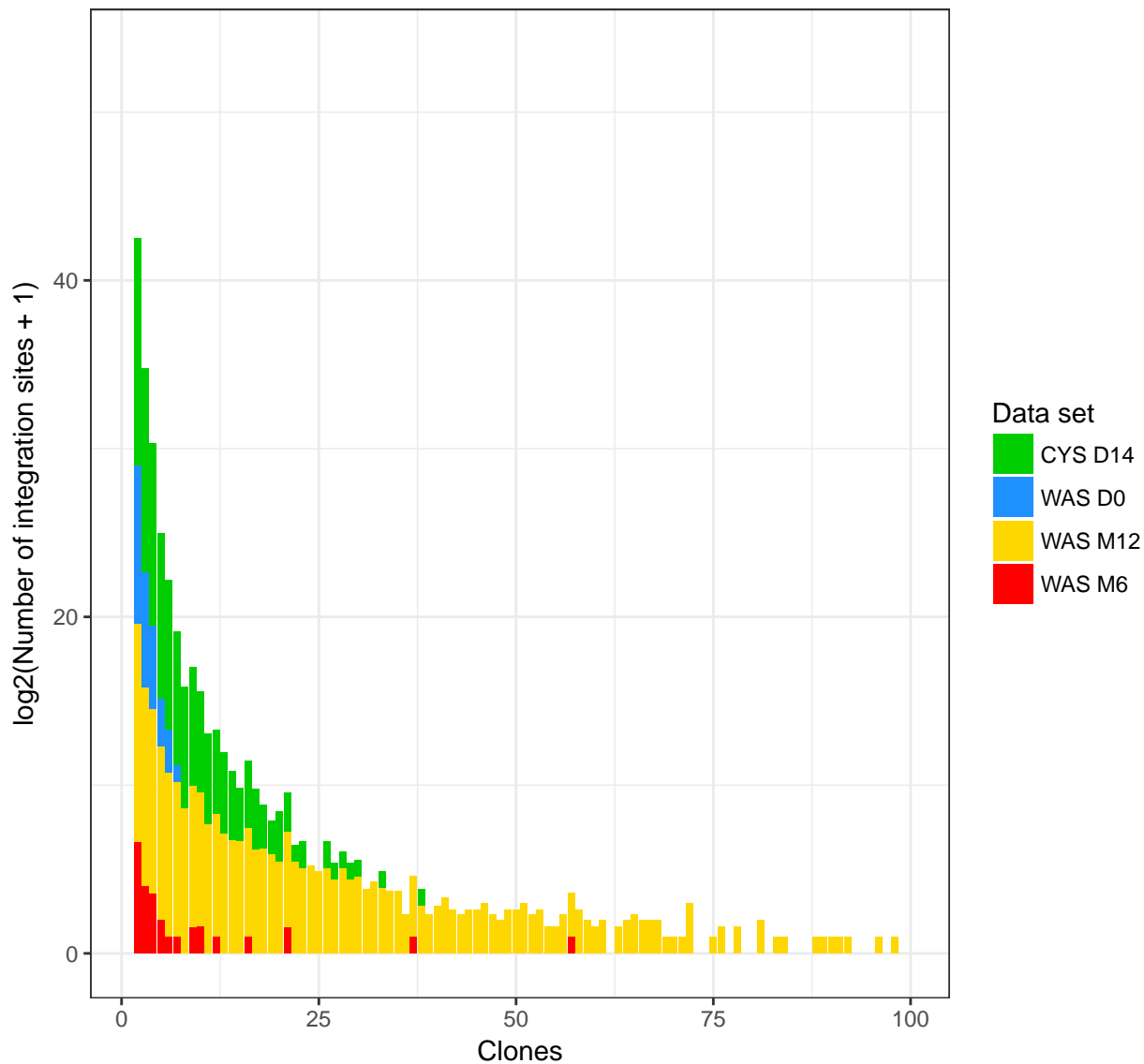
Table S2.

SpecimenAccNum	CellType	Patient	Timepoint	SpecimenInfo
GTSP0688	PBCD34-mock	pCYS002NS	d14	Mock transduced control; Stage: Mock
GTSP0690	PBCD34-mock	pCYS004BR	d14	Mock transduced control; Stage: Mock
GTSP0828	Mouse_BM	pMouseCNL1group1	m6	pCCL-CTNS; MOI 10; Stage: Primary
GTSP0834	Mouse_Sca1pos	pMouseCultureControl	d14	Control, DNA was extracted from mouse Sca1+ cells and cultured for 2 weeks (Mock); Stage:
GTSP1684	PB_CD34	pCYS_017_BW MOCK	d14	Mock transduced control; Stage: Mock
GTSP1693	PB_CD34	pDON.004.3.TL.MOCK	d14	Mock transduced control; Stage: Mock
GTSP1711	T-Cells	pCNL59	m6	Mouse Thymus, T cells
GTSP1868	Bone Marrow	pCN748	m6	"pCCL-CTNS transduced, Secondary graft, Primary graft mouse: CN671, Primary graft VCN: 1.31"
GTSP1975	DNA	pCN752P1	6m	"Mouse, ""growth"" P=pathology sample 1 from CN752 (found in thorax) labelled ""Growth"""
GTSP1976	DNA	pCN752P2	6m	Mouse P=pathology sample 2 from CN752(thymus)

Comparison of the number of integration sites and inferred cells

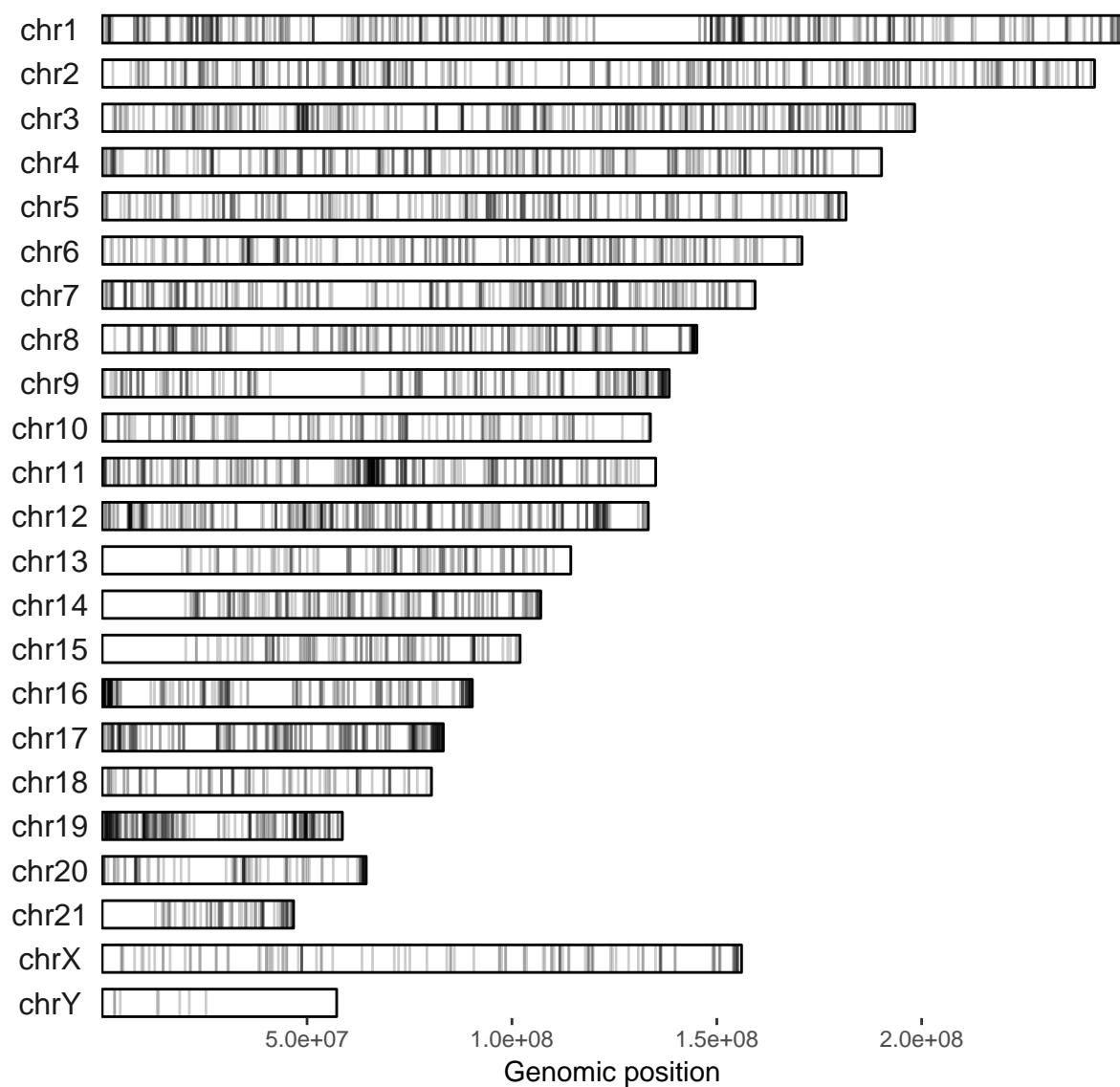
Kolmogorov–Smirnov tests show no significant differences between the distributions of estimated abundances between trials. The plot below was truncated at 100 inferred cells for clarity which eliminated 16 data points from the ‘WAS m12’ distribution.

Figure S1.



Integration positions of the lentiviral therapeutic vector from a previous WAS correction trial¹

Figure S2.



Persistence of clones in mouse BM transplant trials

Table S3.

Donor	Recipient	intSite	Donor cells	Recipient cells
pMouseCNL24group4	pMouseCNL58	chr2+141127890	1,796	3
pMouseCNL25group4	pMouseCNL59	chr2-52586749	7	25
pMouseCNL25group4	pMouseCNL59	chr2-52586682	1	23
pMouseCNL25group4	pMouseCNL59	chr2+52586806	1,764	525
pMouseCNL25group4	pMouseCNL59	chr3-71430231	2	8
pMouseCNL25group4	pMouseCNL59	chr3-59165408	2,907	690
pMouseCNL25group4	pMouseCNL59	chr3+59165404	1	1
pMouseCNL25group4	pMouseCNL59	chr3+59165421	26	134
pMouseCNL25group4	pMouseCNL59	chr3+59165479	6	19
pMouseCNL25group4	pMouseCNL59	chr3+71430357	1,907	260
pMouseCNL25group4	pMouseCNL59	chr9+15188460	1,838	375
pMouseCNL25group4	pMouseCNL59	chr12-55631198	3	1
pMouseCN493	pMouseCNL78	chr6-10697710	2,161	10
pMouseCN493	pMouseCNL78	chr14+15556797	1,769	11
pMouseCN493	pMouseCNL78	chrX-155983905	1,445	10
pMouseCN493	pMouseCNL78	chrX-111592392	2,375	9
pMouseCN540group10	pMouseCN586	chr9-35113079	1	1
pMouseCN552group11	pMouseCNL79	chr12-3110022	10	1
pMouseCN529group11	pCNL80	chr3+123970190	221	37
pMouseCN529group11	pCNL80	chr10-72070385	235	18
pMouseCN529group11	pCNL80	chr16-44221895	246	17
pMouseCN529group11	pCNL80	chrX+9345454	226	18

Sequencing depth

Identified integration site are shown as colored squares that are positioned by the number of reads leading to their identification.

Figure S3.

